Computers & Geosciences 45 (2012) 87–97

Contents lists available at SciVerse ScienceDirect

Computers & Geosciences

journal homepage: www.elsevier.com/locate/cageo

SolEx: A model for mixed COHSCl-volatile solubilities and exsolved gas compositions in basalt

Fred Witham [a,*], Jonathan Blundy [a], Simon C. Kohn [a], Priscille Lesne [a], Jacqueline Dixon [b], Sergey V. Churakov [c], Roman Botcharnikov [d]

[a] School of Earth Sciences, University of Bristol, Queen's Road, Bristol BS8 1RJ, UK
[b] University of South Florida, College of Marine Science, St. Petersburg, FL 33701, USA
[c] Paul Scherrer Institute, 5232 Villigen, Switzerland
[d] Institut für Mineralogie, Universität Hannover, 30167 Hannover, Germany

ARTICLE INFO

Article history:
Received 3 May 2011
Received in revised form
25 September 2011
Accepted 26 September 2011
Available online 29 October 2011

Keywords:
Solubility
Basalt
Sulphur
Chlorine
Water
Carbon dioxide

ABSTRACT

We present a software application, SolEx, to calculate basaltic melt and coexisting vapour compositions in the system C–O–H–S–Cl. Such a model has great utility in interpreting emitted gas and melt inclusion compositions, especially through the incorporation of sulphur and chlorine, the most commonly measured volcanic gas species. We assume that the behaviour of the fluid phase is controlled by the volumetrically dominant volatile species, H_2O and CO_2, whereas sulphur and chlorine partition between the melt and fluid phases. Melt–fluid partition coefficients for S and Cl were parameterised from measurements by Lesne et al. (2011a, p. 1737). The model of Churakov and Gottschalk (2003a, p. 2415) was applied to calculate fugacity coefficients and the equilibrium constants for the reaction $i_{melt} \rightarrow i_{fluid}$ were thereby deduced. SO_2 dominates at oxidation states of $\Delta NNO > 0.5$ (Jugo et al., 2010, p. 5926), where this model is applicable.

In the forward model, total volatile inventories and melt composition are specified by the user. The parameterisation of Dixon (1997, p. 368) is used to predict the partitioning of CO_2 and H_2O between vapour and melt phases. An iterative procedure is employed to predict the partitioning of S and Cl components between fluid and melt phases. Melt and gas compositions and gas volume fraction are thereby modelled over pressures in the range 5–4000 bar. This approach satisfactorily reproduces independent literature data on S and Cl behaviour in basalt. SolEx is a user-friendly software package available for OS X and Windows, facilitating modelling of closed- and open-system C–O–H–S–Cl degassing in basalts.

1. Introduction

The behaviours of water and carbon dioxide fluids in basaltic melts have been well studied (Dixon et al., 1995; Dixon, 1997; Moore et al., 1998; Papale, 1999; Papale et al., 2006; Lesne et al., 2011b, 2011c). The compositions of emitted volcanic gases have been shown to correlate with different styles of volcanic activity (Spilliaert et al., 2006b; Edmonds and Gerlach, 2007), so the combination of thermodynamic or empirical models of volatile solubilities in melts with studies of volcanic gas emissions is a promising avenue for the prediction of volcanic activity (Aiuppa et al., 2007; Aiuppa, 2009). Unfortunately, H_2O and CO_2, the two best-modelled volatile species in melts, are the hardest to measure in emissions due to their relatively high abundances in the atmosphere. Sulphur is the most widely measured species, due to its low atmospheric concentrations and strong absorption of ultra-violet light. Measurements are typically done either with correlation spectroscopy (COSPEC, Millan et al., 1969), or now more regularly with Differential Optical Absorption Spectroscopy (DOAS, Platt, 1994) or FLYSPEC correlation spectroscopy (Horton et al., 2006). Halogen/sulphur ratios, particularly involving chlorine, are often measured using Fourier transform infrared spectroscopy (FTIR, Francis et al., 1998), electrochemical sensors (Aiuppa et al., 2009) or filter packs (e.g. Martin et al., 2010). Aiuppa et al. (2004) suggested that emitted S/Cl ratios correlated with magma degassing style, and Burton et al. (2007) proposed that the composition of gas slugs measured at Stromboli was dependent on the depth at which the slugs became chemically isolated from the magma. Measurements of volatiles, both in emitted gases and melt inclusions trapped within crystals, therefore have the power to further constrain degassing mechanisms, and provide another test for model predictions. A detailed

* Corresponding author. Tel.: +44 7968 894942.
E-mail address: fredwitham@yahoo.co.uk (F. Witham).

0098-3004/$ - see front matter © 2011 Elsevier Ltd. All rights reserved.
doi:10.1016/j.cageo.2011.09.021

model of S and Cl behaviour in H_2O- and CO_2-bearing basaltic melts is highly desirable in order to better understand volcanic gas emissions, and to test models of degassing processes.

We aim to complement the aforementioned studies by developing a model of COHSCl volatile behaviour that is applicable to basalts over a wide range of volcanologically relevant conditions. After calibrating and testing the COHSCl model on one of the basalts studied by Lesne et al. (2011a), we compare our results to both of their experimentally studied basalts, and to the studies of Moretti and Papale (2004), Moune et al. (2009), Stelling et al. (2008), Chevychelov et al. (2008) and Alletti et al. (2009) in order to assess to what extent our model is applicable over a wider spectrum of compositions, oxygen fugacities and temperatures.

1.1. H_2O and CO_2 models

The reader looking for models of H_2O–CO_2 behaviour in silicate melts is already relatively well catered for. Dixon and Stolper (1995) present the most widely cited model of mixed H_2O–CO_2 behaviour, based on a series of experiments on basaltic liquids (Dixon et al., 1995). Dixon (1997) utilised a 7-component parameterisation of composition:

$$\Pi = -6.50(\mathrm{Si}+\mathrm{Al})+20.17(\mathrm{Ca}+0.8\mathrm{K}+0.7\mathrm{Na}+0.4\mathrm{Mg}+0.4\mathrm{Fe}), \quad (1)$$

where Si, etc. represent molar concentrations of the elements. The computer program VolatileCalc (Newman and Lowenstern, 2002) is based upon this parameterisation. Newman and Lowenstern (2002) use the observed dependence of Π on SiO_2 concentration for the North Arch Volcanic field (Dixon et al., 1997) to reduce the parameterisation from 7 components to SiO_2 concentration only. Due to its ease of use, VolatileCalc is probably the most frequently used mixed H_2O–CO_2 solubility calculator at present. However, Lesne et al. (2011c) show that neglecting the effect of alkalis on CO_2 solubility (i.e. by reducing the Π parameterisation to SiO_2 only) leads to VolatileCalc overestimating saturation pressures by up to 50% in melts from Vesuvius. Similar discrepancies arise for many alkaline volcanic suites (e.g. Vetere et al., 2011). It is therefore very important to include the full 7-component Π parameterisation in models of COH solubility.

An independent approach was taken by Papale (1999) and later refined by Papale et al. (2006). They performed a multivariate regression upon all published CO_2 and H_2O solubility data (subject to considerations regarding the accuracy and validity of each experimental approach used), and produced a model based on 29 parameters and calibrated over a remarkably wide range of melt compositions and P–T conditions. Unfortunately, whilst there are numerous studies of water solubility in basalt, there are still insufficient measurements of CO_2 solubility to form a robust model of CO_2 or mixed H_2O–CO_2 behaviour over all volcanologically relevant conditions. The controversial nature of the CO_2 data is evidenced by the fact that the increase of almost 100% in the size of the experimental database between Papale (1999) and Papale et al. (2006) had a negligible impact on H_2O results but changed the CO_2 results dramatically (Papale et al., 2006). The model of Papale et al. (2006) is available in the form of a web-based calculator from http://ctserver.ofm-research.org/Papale/Papale.php.

A review by Moore (2008) details other models of H_2O and CO_2 solubilities in basaltic melts. Moore's conclusion is that if one wishes to calculate mixed H_2O–CO_2 solubilities, Dixon's (1997) model works best for tholeiitic melts, whereas Papale et al. (2006) is best for calc-alkaline magmas. We here compare the performance of Dixon's (1997) model with experiments from the literature; experimental melt compositions are given in Table 1. Fig. 1a shows that the model of Dixon (1997) provided a good fit to the experimental data of Lesne et al. (2011a), whereas that of Papale et al. (2006) significantly overestimates CO_2 contents of the melt at pressures greater than 2.5 kbar. Shishkina et al. (2010, Fig. 7) found an overestimation of pure CO_2 solubility by the Papale et al. (2006) model. Despite the underestimation of total volatile solubility at >3 kbar shown in Fig. 1b, which Shishkina et al. (2010) ascribe to non-Henrian behaviour at pressures above 2 kbar, they found the Newman and Lowenstern (2002) implementation of Dixon (1997) to be a better description of their results. Fig. 1c shows the excellent agreement of Dixon (1997) with data from Pichavant et al. (2009) at <3 kbar. Here we again find an underestimation of total COH solubility at 4 kbar. Good agreement between experiments and Dixon's (1997) model was also found for pure H_2O (Lesne et al., 2011b) and CO_2 (Lesne et al., 2011c) solubilities in melts of compositions matching those found at Vesuvius, Stromboli and Etna volcanoes. Given its success, in particular at pressures ≤ 2 kbar where most degassing occurs, we employ the model of Dixon (1997) to model COH solubility in SolEx.

Fig. 1d shows that COH solubilities reported from Vetere et al. (2011) are significantly underestimated by the model of Dixon (1997). Comparison with their Fig. 7 shows that the Papale et al. (2006) model provides a better description of their data at >2 kbar, whereas Dixon (1997) is still the better model at lower pressures. Despite being the most alkalic melt tested here (Table 1), it is well within the range of total alkalis used to calibrate the Π parameterisation (Dixon, 1997). The only major element outside the calibrated range for Π is Si. Given the good agreement for <52 wt% SiO_2 (St8.1, Fig. 1), we therefore discourage applying the Dixon (1997)

Table 1
Compositions and experimental conditions of basalts studied.

	SiO_2	TiO_2	Al_2O_3	FeO	Fe_2O_3	MgO	CaO	Na_2O	K_2O	Π	T (°C)
St8.1[a]	52.12	0.88	16.38	5.82	3.00	6.71	10.72	2.47	1.89	−0.053	1150
MAS1[a]	52.86	1.25	15.51	9.47	3.86	3.95	8.49	3.08	1.52	−0.508	1150
N72[b]	50.17	0.92	18.28	4.22	5.15	7.00	11.37	2.33	0.23	−0.377	1250
PST-9[c]	50.2	0.84	15.2	6.87	0.94	7.87	12.4	2.29	1.86	0.641	1150
Shoshonite[d]	53.47	0.71	15.48	3.36	5.03	4.88	8.51	3.66	4.72	−0.052	1250
OIB[e]	49.16	2.29	13.33	9.71	1.31	10.41	10.93	2.15	0.5	0.710	
n-MORB[f]	49.51	0.90	16.75	8.05		9.74	12.50	2.18	0.065	0.205	
Shoshonite2[g]	47.8	0.98	16.5	5.88	1.96	4.42	12.5	2.42	1.73	0.281	1145

[a] Lesne et al. (2011a).
[b] Shishkina et al. (2010).
[c] Pichavant et al. (2009), FeO/Fe_2O_3 ratio calculated using the model of Kilinc et al. (1983) using $\Delta NNO = +3.5$, the average reported from experiments at 884 bar and 2010 bar.
[d] Vetere et al. (2011).
[e] Ocean island basalt, the 1921 Kilauea lava of Yoder and Tilley (1962).
[f] n-MORB average composition of Presnell and Hoover (1987), FeO is assumed to equal total Fe.
[g] Shoshonite of Moretti and Papale (2004), here calculated with $FeO/Fe_2O_3 = 3$.

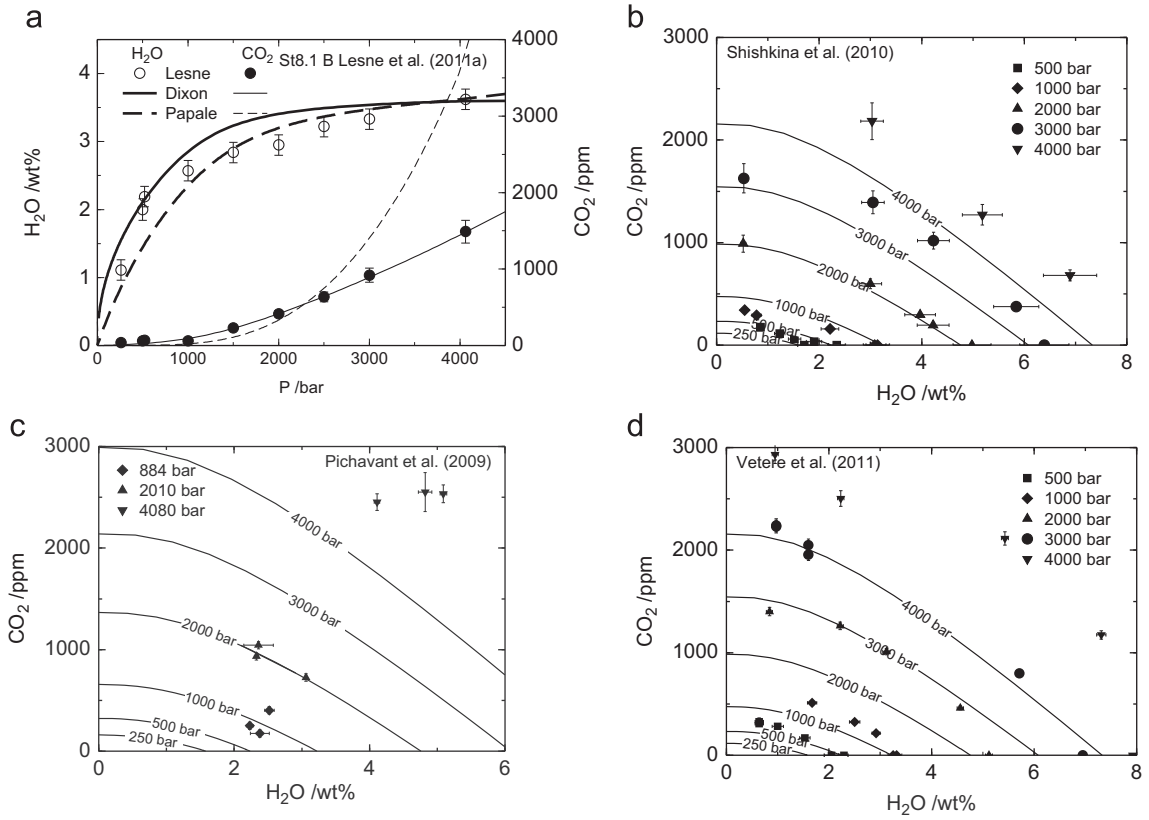

Fig. 1. (a) A comparison of the models of Dixon (1997) and Papale et al. (2006) with experimental data on the St8.1 basalt from Lesne et al. (2011a). Experiments are at 1150 °C and for a fixed bulk composition (Table 1). The Papale et al. (2006) model overestimates dissolved CO_2 concentrations measured in these experiments. (b–d) A comparison of the Dixon (1997) model with data from Shishkina et al. (2010), Pichavant et al. (2009) and Vetere et al. (2011).

model of COH solubility, and therefore SolEx, to melts with SiO_2 concentrations greater than 53 wt%.

1.2. Sulphur models

Despite playing an important role in degassing processes, few data are available on the solubilities of S and Cl in hydrous silicate melts in equilibrium with COHSCl fluids. Data for basaltic systems are even more sparse, largely due to difficulties in obtaining experimental data at high temperature and controlled oxygen fugacity (Moune et al., 2009). Sulphur solubilities in basalt have been parameterised at 1 atm (Wallace and Carmichael, 1992) and at 1 GPa and high T (Jugo et al., 2005; Liu et al., 2007) as a function of temperature and oxygen and sulphur fugacities (f_{O_2} and f_{S_2}) assuming saturation in a liquid sulphide phase. Wallace and Carmichael (1992) found that sulphur dissolves as S^{-2} for redox conditions beneath the Quartz–Fayalite–Magnetite buffer and as S^{+6} at $\Delta NNO > +1.2$, where ΔNNO is the difference in oxygen fugacity (in log units) from the nickel–nickel oxide buffer. In the range $0.8 < \Delta NNO < 1.2$ there is a rapid change in S speciation. These results are in broad agreement with those of Jugo et al. (2010) who found a change in S speciation in the range $-1 < \Delta NNO < 1$, with most of the change occurring in $-0.5 < \Delta NNO < 0.5$ (Fig. 2).

Scaillet and Pichavant (2005) developed an empirical model of COHS fluid behaviour in basalts. They combined numerous experimental datasets, spanning a range of compositions between intermediate and basaltic magma compositions. However, their model of sulphur fugacity is only correct to within an order of magnitude (Scaillet and Pichavant, 2005), which in turn causes a large uncertainty in predicted S concentrations within magmas. Moretti et al. (2003) and Moretti and Papale (2004) have produced a thermodynamic model for COHS fluid behaviour, based

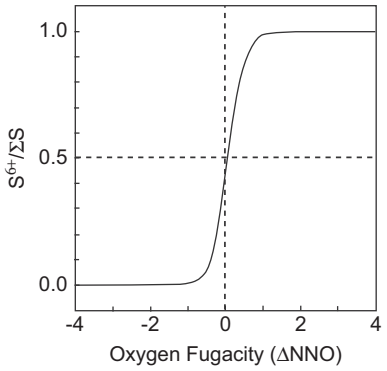

Fig. 2. Sulphur speciation as a function of oxygen fugacity, after Jugo et al. (2010), showing that S is dominantly present as S^{+6} (SO_4^{2-}) when $\Delta NNO > 1$ and as S^{-2} (H_2S) when $\Delta NNO < -1$.

on the Belonoshko et al. (1992) model of fugacities in fluids with complex compositions, assuming that the magma remains undersaturated in any liquid or solid sulphur-bearing phases. By virtue of being calibrated over a wide range of compositions, the approaches taken by Moretti et al. (2003), Moretti and Papale (2004) and Scaillet and Pichavant (2005) can lose precision for a given magma composition but their thermodynamic basis gives increased confidence in extrapolations. Moretti and Papale (2004) were able to reproduce observed solubility features and describe high pressure data well (Moretti and Ottonello, 2005). An interesting corollary of these studies is that they suggest up to 5 wt% of magma at Stromboli, Etna, Vulcano and Vesuvius volcanoes could be a free COHS fluid phase (Scaillet and Pichavant, 2005). Such a high value requires a reduction in estimates of the volumes of

degassed magma that must be intruded at depth to account for the observed emitted sulphur fluxes from these volcanoes (e.g. Allard et al., 1994).

1.3. Chlorine models

Studies on rhyolitic systems have been carried out for COHCl (Webster, 1997; Webster and Rebbert, 1998) and HOSCl (Botcharnikov et al., 2004). Webster (1997) found that the addition of CO_2 caused a small increase in the solubility of Cl, which has been ascribed to an increase in the immiscibility gap between the hydrous and brine fluid phases (Shmulovich and Graham, 2004). Such strongly non-ideal behaviour of the fluid has also been observed in andesitic (Botcharnikov et al., 2007) and phonolitic and trachytic (Webster et al., 2009) systems. Carroll (2005) gives a review of Cl-bearing fluid behaviours in evolved alkaline magmas, and notes that Cl solubility can increase with decreasing pressure.

Webster et al. (1999) and Webster (2004) showed that basaltic HOCl fluids do not display immiscibility at Cl concentrations of less than 2 wt%, while Stelling et al. (2008) found the onset of immiscibility at [Cl] > 3 wt%. Webster et al. (1999) found that Cl solubility in basaltic systems is only weakly pressure dependent, but is a function of melt composition, with more mafic melts having higher solubilities. Furthermore, the bulk Cl concentrations of most basaltic and andesitic magmas are substantially less than those required for saturation in a Cl-rich brine phase (Webster and de Vivo, 2002). Instead, the exsolution of CO_2–H_2O dominated vapours will dictate Cl (and S) behaviours, with Cl partitioning into that phase. We describe partitioning by the use of the partition coefficient $D_i^{fl-m} = [i]^{fl}/[i]^m$, where $[i]$ is the mass concentration of species i in the fluid (fl) and melt (m). Webster et al. (1999) report values of D_{Cl}^{fl-m} between COHCl fluid and andesitic and basaltic melts at $P = 2$ kbar and $T = 1100$ °C of between 0.9 and 6, and for coexisting fluids with 1 wt% and 11 wt% Cl, respectively. This dependence of D_{Cl}^{fl-m} on fluid composition suggests that the COHCl gas is not behaving ideally.

Chlorine partitioning is complicated further by the presence of several chloride species, HCl, NaCl and KCl being foremost among them. At high pressure Cl behaviour is dominated by NaCl exchange reactions (Burnham, 1979), whereas HCl is the dominant aqueous chloride-bearing phase at low pressure. The combination of exchange reactions leads to complicated, non-linear effects on chlorine partitioning (Shinohara, 2009, and references therein). For example, HCl dissolves in silicate melts by reacting with O^{2-} ions in the melt to form OH^- and Cl^- (Burnham, 1979). OH^- is related to the dissolution of H_2O, meaning so there is interaction between H_2O and HCl behaviours over and above the partitioning behaviour modelled in this study. Furthermore, Na and K contents of the melt will affect the stabilities of other chlorides (Shinohara, 2009). All such effects are beyond the scope of this work. We highlight that the dominant Cl-bearing phase at low pressure is HCl, and suggest that given the paucity of aqueous brine phases in the basalts of interest, the combined effects of chloride salt species are of secondary importance to the partitioning behaviour we describe.

Alletti et al. (2009) parameterised the partition coefficient of Cl between melt and COHCl fluids in equilibrium with basalts from Etna at $\Delta NNO = 0$ and $\Delta NNO = +2$. They found that the partition coefficient, D_{Cl}, in HOCl bearing systems, with 0.1–2 wt% Cl and $T = 1260$ °C, has values of 35–6 with a negative pressure dependence, in accordance with the studies reported by Carroll (2005) in alkaline magmas. The addition of CO_2 to the system seems to remove the pressure dependence, and reduces the value of D_{Cl} by approximately 50%. Results from Alletti et al. (2009) are not significantly affected by oxidation state of the melt over the studied range of $0 < \Delta NNO < +2$.

Stelling et al. (2008), also working on Etnean basalts and at temperatures of 1050–1250 °C, reported similar values of $0.04 < D_{Cl} < 24$, with $D_{Cl} < 1$ for total Cl concentrations of < 1 wt%—the range found in basaltic melts. They noted a distinct dependence of D_{Cl} on fluid composition. Such composition-dependent behaviour indicates that the fluids are not behaving ideally.

The use of a specific composition of basalt gives confidence when recreating Etnean processes, though raises the question of how applicable the study is to other volcanoes, given that Cl solubility is dependent on silicate magma composition (Métrich and Rutherford, 1992; Webster et al., 1999).

2. Modelling approach

Sulphur and chlorine form relatively minor components in typical basaltic volatile inventories, subordinate to water and often to carbon dioxide (e.g. Dixon et al., 1991; Webster et al., 1999 and references therein; Métrich et al., 2001; Hauri, 2002; Spilliaert et al., 2006a; Sadofsky et al., 2008; Collins et al., 2009). Given the relatively low S and Cl contents of typical basaltic melts, we suggest that their behaviour can be modelled with a standard trace-element approach. That is, we assume that the concentrations of S and Cl do not affect the behaviour of the volumetrically dominant volatile components, H_2O and CO_2. This assumption is in agreement with the findings of Wallace and Carmichael (1992), who concluded that as magma ascends, H_2O and CO_2 begin to exsolve due to the decrease in pressure, and a certain proportion of S fractionates into the vapour so that its concentration in the melt is progressively depleted.

We therefore use existing models of H_2O and CO_2 behaviour to describe the fluid phase, and determine partition coefficients, D_i^{fl-m}. The partition coefficient may be a function of fluid composition (e.g. Stelling et al., 2008), so it is desirable to model the equilibrium constant, K_i, of the reaction $i_{fl} \rightarrow i_m$:

$$K_i = \frac{f_i^{fl}}{a_i^m} = \frac{\Gamma_i^{fl} P X_i^{fl}}{\gamma_i^m X_i^m} = \frac{\Gamma_i^{fl} P [i]^{fl} \lambda}{\gamma_i^m [i]^m} = \frac{\Gamma_i^{fl} P D_i \lambda}{\gamma_i^m}, \quad (2)$$

where f_i^{fl} is the fugacity of i in the fluid, a_i^m is the activity of i in the melt, Γ_i^{fl} is the fugacity coefficient of i, γ_i^m is the activity coefficient of i, X_i is the molar concentration of i in fluid or melt, P is the pressure in bar and λ is the ratio of fluid molar mass to melt molar mass. We define melt and fluid molar masses as the weighted means of the molar masses of their component oxides (and chloride in the case of HCl). Γ_i^{fl} and γ_i^m are assessed in Section 3.2, and K_i is parameterised in Section 3.3.

3. Algorithms employed in SolEx

3.1. COH behaviour

The model of Dixon (1997) is based on the Modified Redlich–Kwong equation of state (Holloway, 1977), though at the modelled pressures (< 4 kbar) and temperatures (~ 1200 °C) differences in fugacities calculated using various alternative equations of state are not significant (Dixon, 1997). The activity of H_2O is taken to be the activity of molecular H_2O in the melt (Holloway and Blank, 1994). The amounts of carbonate and molecular H_2O dissolved in tholeiitic melts coexisting with pure carbon dioxide or H_2O vapour at 1200 °C can be calculated from the following equations (Dixon et al., 1995):

$$X_{CO_3^{2-}}^m(P,T_0) = X_{CO_3^{2-}}^m(P_0,T_0) \frac{f_{CO_2}(P,T_0)}{f_{CO_2}(P_0,T_0)} \exp\left[\frac{-\Delta V_r^{0,m}(P-P_0)}{RT_0}\right] \quad (3)$$

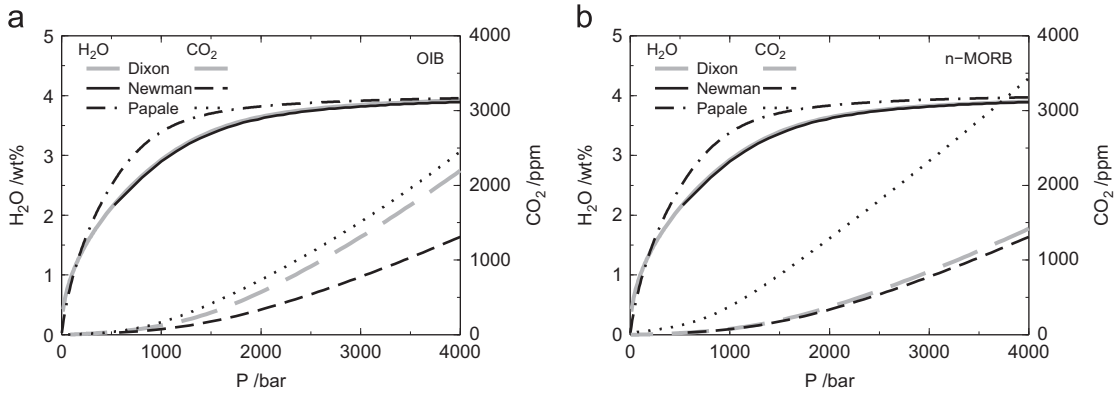

Fig. 3. A comparison of the COH-solubility model of Dixon (1997), upon which this work is based, with those of Newman and Lowenstern (2002) and Papale et al. (2006), for typical ocean island (OIB) and mid-ocean ridge (n-MORB) basalts (see Table 1 for compositions). Comparisons are for a closed system 4 wt% H_2O and 5000 ppm CO_2 at 1150 °C. There is good consistency between different models of H_2O behaviour, but CO_2 profiles exhibit significant variability.

and

$$X^m_{H_2O,\mathrm{mol}}(P,T_0) = X^m_{H_2O,\mathrm{mol}}(P_0,T_0)\frac{f_{H_2O}(P,T_0)}{f_{H_2O}(P_0,T_0)}\exp\left[\frac{-V^{0,m}_{H_2O}(P-P_0)}{RT_0}\right], \quad (4)$$

where $X^m_i(P,T_0)$ is the mole fraction of carbonate or molecular H_2O in melt saturated with vapour with a fugacity of carbon dioxide or water of $f_i(P,T_0)$ at pressure, P, and temperature, $T_0 = 1473.15$ K; $P_0 =$ 1 bar; $f_i(P_0,T_0) = 1$ bar; $X^m_{CO_3}(P_0,T_0) = 3.8\times10^{-7}$ and $X^m_{H_2O}(P_0,T_0) = 3.28\times10^{-5}$ (Dixon, 1997); $V^{0,m}_{H_2O}$ is the molar volume in the standard state and is assumed to be constant and equal to the partial molar volume of H_2O in the melt (12 $cm^3\,mol^{-1}$; Dixon et al., 1995); $\Delta V^{0,m}_r = V^{0,m}_{CO_3} - V^{0,m}_{O_2} = 23\ cm^3\ mol^{-1}$ (Pan et al., 1991) and $V^{0,m}_{CO_3}$ and $V^{0,m}_{O_2}$ are the molar volumes of the melt species in their standard states and have been taken to be independent of P and T in deriving Eq. (3) (after Pan et al., 1991) and R is the gas constant (83.15 $cm^3\,bar\,mol^{-1}\,K^{-1}$).

A regular solution model (Silver and Stolper, 1989) is used to calculate the concentration of hydroxyl groups in the melt. The mole fraction of total H_2O dissolved in the melt, $X_B = X_{H_2O} + X_{OH^-}/2$, is calculated and the mass fraction of H_2O in the melt is given by $[H_2O]/\mathrm{wt\%} = 1801.5X_B/(36.6-18.6X_B)$.

Carbonate solubility is strongly dependent on melt composition, which is parameterised as Π (Section 1.1), but negligibly dependent on temperature (Pan et al., 1991). The molar proportion of carbonate at reference conditions P_0, T_0 is given by

$$X_{CO_3^{2-}} = 7.94\times10^{-7}(\Pi + 0.762) \quad (5)$$

and converted to a mass fraction by

$$[CO_2]/\mathrm{ppm} = 10^4[4400X_{CO_3^{2-}}/(36.6-44X_{CO_3^{2-}})]. \quad (6)$$

Assuming that CO_2 and H_2O dominate the vapour phase and that these species mix ideally, then, following Dixon et al. (1995), at vapour saturation the activities, a, of the species satisfy

$$a^m_{H_2O}/a^{0,m}_{H_2O} + a^m_{CO_3^{2-}}/a^{0,m}_{CO_3^{2-}} = 1 \quad (7)$$

and

$$a^m_{H_2O}/a^{0,m}_{H_2O} = X^{fl}_{H_2O}, \quad (8)$$

$$a^m_{CO_3^{2-}}/a^{0,m}_{CO_3^{2-}} = X^{fl}_{CO_2}. \quad (9)$$

The denominators of Eq. (7) are constant for a given melt composition, P and T. The model can then be iterated, sequentially moving more volatile from fluid to melt, until equilibrium is achieved.

This implementation is very similar to that of Newman and Lowenstern (2002), but with the addition of the full 7-component parameterisation of composition. We also calculate iteratively from the no-exsolved-vapour condition to find the equilibrium vapour composition for each pressure, rather than using the solution at each pressure as a starting point for the next pressure. The partitioning behaviour is a function of pressure, so this solution scheme results in a modest increase in accuracy compared to Newman and Lowenstern (2002). Fig. 3 shows a comparison between the results of Newman and Lowenstern (2002), Papale et al. (2006) and this study for a typical ocean island basalt (OIB, a 1921 lava from Kilauea, Hawaii, studied by Yoder and Tilley, 1962) and mid-ocean ridge basalt (an average n-MORB composition from Presnell and Hoover, 1987, previously used by Workman and Hart, 2005); compositions are given in Table 1. The H_2O behaviour is similar in all three models, but significant variability is shown in CO_2 solubility. We point out that SolEx behaves similarly to the model of Papale et al. (2006) in the OIB example and similarly to that of Newman and Lowenstern (2002) for n-MORB; SolEx is close to the best available model (as identified by Moore, 2008) in both cases. This suggests that SolEx is appropriate for use on a wide range of basaltic compositions.

3.2. Non-ideality of fluid and melt phases

Churakov and Gottschalk (2003a,b) present a model based on a perturbation theory to generate equations of state (EOS) that can be used for any given volatile species. The advantage of this approach is that complex mixtures can be treated (because all the species have the same form of EOS, simple mixing rules can be applied), provided that the relevant data (Lennard–Jones potential coefficients, polarisability and dipole moments) are available. We use their mixed fluid model to calculate fugacity coefficients for H_2O, CO_2, SO_2 and HCl in the fluid phase. By calculating fugacities we can account for the non-ideality of the fluids, and calculate equilibrium constants from measured partition coefficients (Eq. (2)).

Lesne et al. (2011a) showed that the partitioning of S is modestly composition dependent, and therefore non-ideal. For example, their Fig. 8 shows that there is a minimum in D^{fl-m}_S of ~1 at 1000–2000 bar in St8.1 melt whereas the minimum is ~5 in MAS1 melt. We note that the non-ideality highlighted by Lesne et al. (2011a) is very close to being within their uncertainties, so, in the interests of simplicity, we therefore assume mixing of S and Cl in the melt to be ideal ($\gamma^m_S = \gamma^m_{Cl} = 1$) on the grounds that its neglection is unlikely to significantly degrade our results.

3.3. Sulphur behaviour under reducing conditions

Various authors have studied the behaviour of sulphur in COHS fluids under reducing conditions. Scaillet et al. (1998) and Keppler (2010) attempted to establish the value of D_S in COHS systems at oxygen fugacities of $\Delta NNO < -1$ for andesitic to rhyolitic systems. We attempted the same exercise from data presented by Moune et al. (2009). However, sulphur tends to precipitate as pyrhotite or an immiscible FeS phase under reduced conditions. Moretti and Baker (2008) show that increasing pressures encourage S into FeS phases, whereas increased H_2O concentrations favour S dissolution in the silicate melt. The combined effect in H_2O-rich basalt is that increased pressure causes more S to be dissolved in the melt as the dissolved H_2O concentration is increased by the increased pressure (Dixon et al., 1995). Moretti and Baker (2008) conclude that, due to changes in oxygen fugacity, H_2O-poor basalts will become undersaturated in FeS phases during isothermal ascent.

The uncertainties inherent in estimating the modal abundance of S-bearing phases and the concentrations of S within them make establishing reliable estimates of D_S highly problematic, and may explain the several orders of magnitude and opposite pressure dependencies observed by Scaillet et al. (1998) and Keppler (2010). Even utilising a subset of experiments described by Moune et al. (2009) as being free of S-bearing solid phases, evidence of S saturation was manifest. In light of these uncertainties, we refrain from using any of the above studies to parameterise the behaviour of an H_2S species. Dedicated experiments are required at S concentrations sufficiently low to prohibit saturation in S-bearing solid phases, over a range of pressures and at f_{O_2} sufficient to maintain most S in the reduced state. We hope to include the results of such studies in future releases of SolEx.

3.4. S and Cl partitioning

We empirically parameterise K_i (Fig. 4) as a function of pressure, P, using the experimental results (St8.1, at 1150 °C, $\Delta NNO = +1.6 - +2.0$ and composition shown in Table 1) reported in Lesne et al. (2011a) for S and Cl. There are large uncertainties in D_i, and so in K_i, because of the mass balance calculations used to establish the composition of the fluids. The mass of each species in the fluid is the difference between the mass added and that in the melt, which is typically (for S and Cl) the relatively small difference between two relatively large numbers. The analytical uncertainties, whilst tolerably small in both initial sample and melt compositions, combine to produce uncertainties of up to (and sometimes exceeding) ±100%. The experiments of Lesne et al. (2011a) were designed to alleviate these problems as much as possible. The consistent trends in the derived values of K_S with pressure give added confidence in their validity.

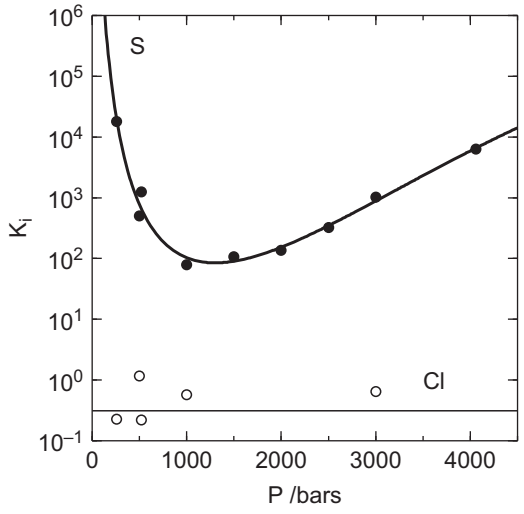

Fig. 4. Empirical parameterisation of K_S and K_{Cl} as functions of pressure, P. Data from Lesne et al. (2011a). The parameterisations are given in Eq. (10). Cl data at 1500, 2000 and 2500 bar are not plotted as all give K_i=0, but are included in the average value plotted on the graph.

Chlorine partition coefficients are of order 1. The small mass of fluid compared to melt means that very little Cl leaves the melt, exacerbating the uncertainties. A value of $D_{Cl} = 0$ is within uncertainty of the results of Lesne et al. (2011a). Volcanoes release significant quantities of HCl, so D_{Cl} must be non-zero. We therefore do not parameterise K_{Cl} as a function of pressure, but simply calculate the average value of D_{Cl}. The success of our model in reproducing melt compositions justifies the approach, but the large uncertainties must be taken into account when modelling coexisting gas Cl contents; further experiments with a larger fluid to melt ratio would help improve the model precision. Low pressure (< 50 bar) experiments would also be of benefit to constrain Cl degassing at near-surface conditions. Despite these shortcomings of the experiments we have confidence in the trends, but absolute values of $[Cl]^{fl}$ may err by hundreds of per cent.

The best-fit values for partition coefficients used in SolEx are

$$\log K_S = 431.69P^{-0.0074946} - 410.49 + 2.7426 \times 10^{-3}P - 1.4891 \times 10^{-7}P^2,$$

$$K_{Cl} = 0.31. \quad (10)$$

The trend in K_S (Fig. 4) merits some comment; K_S is large at low pressures and decreases with increasing pressure. This conforms with expectation; at constant T, the Gibbs free energy equation takes the form:

$$\frac{\delta \ln K_i}{\delta P} = -\frac{\Delta V_i}{RT}, \quad (11)$$

so a negative gradient is predicted for positive ΔV. K_S has a minimum at ~1000 bar, and then increases with increasing pressure. Effects in the fluid are taken account of in the modelling of the fugacity coefficient, so the minimum in K_S must be controlled by the melt phase. Lesne et al. (2011a) carefully assessed the oxidation state of their melts, and have ruled out a changing oxidation state of the melt (as H_2O is dissolved/exsolved), and consequent change in S speciation, as a source of this behaviour. We speculate that there is a change in coordination or complexation of SO_4^{2-} in the melt phase at ~1 kbar that gives rise to this change. If such a change is dependent on the H_2O–CO_2 content of the melt, then the parameterisation will change as total volatiles change. This is not accounted for in the current model, and there are insufficient relevant independent datasets to test this. The agreement with the model of Moretti and Papale (2004) is probably the best cause for confidence that this is not a large effect.

4. Evaluation of performance

The H_2O–CO_2 calculations in SolEx are calibrated over a wide range of basaltic and alkali-basalt compositions, spanning nephelinites, tholeiites and ocean island basalts. The parameterisations of fugacity coefficients (Churakov and Gottschalk, 2003a,b) are applicable over the full range of fluid compositions modelled. The S and Cl partitioning algorithms have been calibrated on a single composition, that of St8.1 (Table 1), for pressures < 4 kbar and temperatures around 1150 °C. It is therefore imperative to test SolEx with independent experiments and at other temperatures and compositions. Unfortunately, there are few experiments in

the literature with S and Cl as dilute components in a fluid phase, as most previous studies have focused on S and Cl solubilities. We have therefore performed our parameterisation on a subset of the data of Lesne et al. (2011a) so that we can use the remainder as independent tests. We also compare our model to the few relevant studies we could find in the literature.

Fig. 5 shows that SolEx reproduces the experimental trends of Lesne et al. (2011a) well for both of their studied compositions. Only the St8.1 B experiments (Table 2) were used in the parameterisation, leaving other experiments to be used as independent tests of the model. The St8.1 B experiments are not reproduced perfectly, despite being the basis of the S–Cl parameterisation, because the parameterisation used measured H_2O and CO_2 concentrations to calculate partition coefficients whereas the model results use the COH solubility model of Dixon (1997) to predict H_2O and CO_2 concentrations within the melt. The discrepancy in St8.1 B comes from the modest imprecision of the COH model. Both S and Cl concentrations within the melt are described to within analytical uncertainty (1σ errors) for all of the experiments of Lesne et al. (2011a), with the exception of some S experiments in the MAS1 B series. Fig. 5c shows that repeated experiments at identical P, T conditions give differing results, i.e. fall outside 1σ errors of each other. This highlights that there is experimental uncertainty in addition to the analytical errors, and illustrates that it is not necessarily the model that is in error here—the mass balance calculations amplify any errors in the experimental technique. There is also a discrepancy in the higher pressure MAS1 A experiments. Although only the 3 kbar experiment falls outside 1σ error of the model, there is what seems to be a systematic offset from the modelled trend. Introducing a compositionally dependent activity coefficient for the melt, γ_m, did not significantly improve the performance of the model overall (Section 3.2), though it did improve the fit here. Improved compositional parameterisation of γ_m would improve the performance of SolEx, but at present we feel there are insufficient experimental data to justify such an approach.

We also compare results from SolEx to the model of Moretti and Papale (2004) and experimental measurements of Stelling et al. (2008), Alletti et al. (2009) and Chevychelov et al. (2008). The latter three studies investigate chloride solubilities in basalts from Mt. Etna, Italy, at a variety of temperatures (1050–1250 °C) and pressures (10–2000 bar). This allows further tests of the compositional and pressure parameterisations for chlorine, and testing of the applicability of the temperature independence assumed in the partitioning behaviour. Fig. 6 shows that SolEx reproduces the experimental chlorine concentrations well over the full range of pressures and temperatures. Results are consistent with the results for S concentration in the shoshonitic melt modelled by Moretti and Papale (2004). Pino et al. (2011) present results from the model of Moretti and Papale (2004) for a Strombolian basalt. The trends of the two models are in general agreement, but results diverge at low

Table 2
Total volatile contents used in the experiments of Lesne et al. (2011a). All experiments were performed at 1150 °C.

Experiment	H_2O (wt%)	CO_2 (ppm)	S (ppm)	Cl (ppm)	ΔNNO
St8.1 A	3.44	4600	1930	2040	1.6–2.4
St8.1 B	3.67	4890	3560	1570	1.6–2.0
St8.1 uncertainty	±0.15	±150	±67	±63	
MAS1 A	2.71	7410	595	1700	0.66–0.75
MAS1 B	2.86	6850	1400	1420	0.68–0.82
MAS1 uncertainty	±0.15	±710	±180	±110	

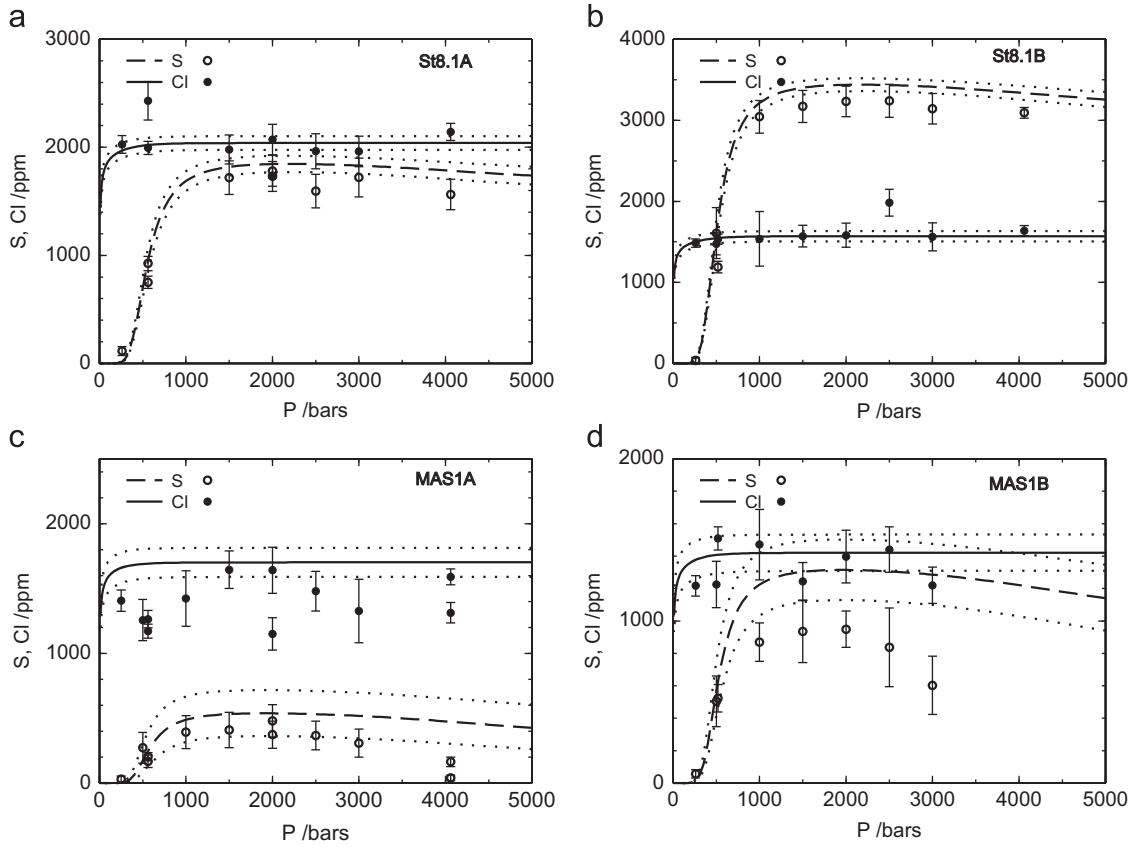

Fig. 5. Comparison of SolEx with experimental data from Lesne et al. (2011a); compositions and experimental conditions given in Table 1 and volatile contents given in Table 2. Error bars represent 1σ uncertainties. Dotted lines show uncertainties on model predictions, based on 1σ analytical uncertainties in starting conditions. Note that only St8.1 B experiments were used to calibrate SolEx.

pressures. The large amount of exsolved CO_2 at low pressures combined with our empirical, compositionally independent model of K_S leads to lower predictions of dissolved S concentration by SolEx.

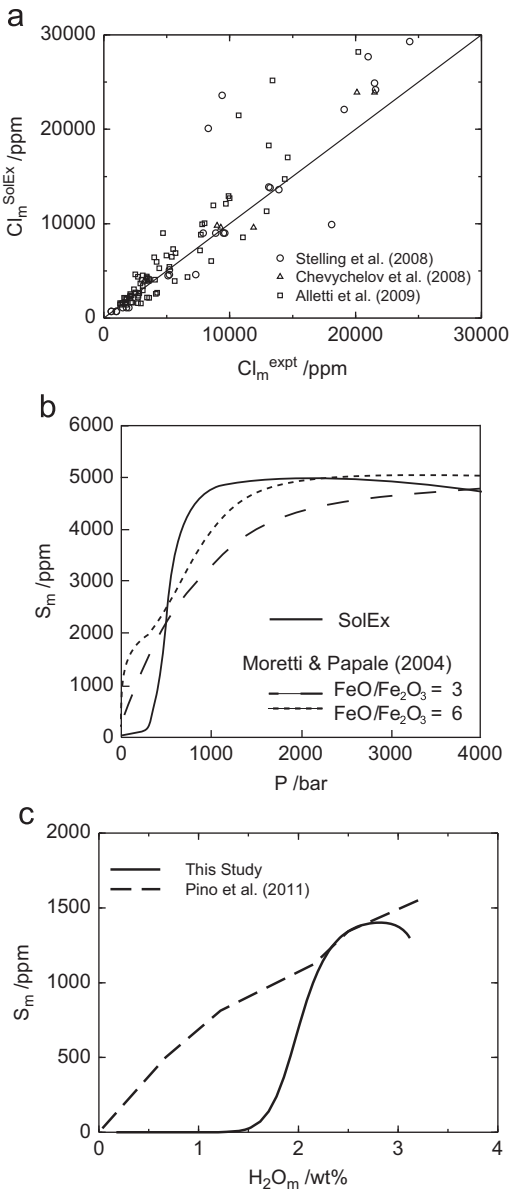

Fig. 6. (a) Comparison of SolEx with experimental data from $P=10$–2000 bar, $T=1200$–1260 °C, $0<\Delta NNO<+2$ (Alletti et al., 2009); $P=2000$ bar, $T=1200$ °C, $\Delta NNO=0$ (Chevychelov et al., 2008) and $P=2$ kbar, $T=1050$–1250 °C, $\Delta NNO=0$ (Stelling et al., 2008). (b) Comparison of SolEx (solid line) with the model of Moretti and Papale (2004) for shoshonitic composition melt (Table 1) with $H_2O=4.0$ wt%, $CO_2=1.0$ wt%, $S=5000$ ppm. (c) Comparison to Moretti and Papale (2004) model results presented by Pino et al. (2011) with composition given in Table 3, $+0.5<\Delta NNO<+1.0$, $H_2O=3.7$ wt%, $CO_2=2.44$ wt%, $S=1500$ ppm.

This reduction in S is due to the big increase in K_S that Lesne et al. (2011a) observe at $P<1000$ bar (Fig. 4). This comparison between the SolEx and the model of Moretti and Papale (2004) emphasises both the reliability of the general trends and the caution with which quantitative model predictions must be interpreted.

No crystallisation was apparent in the preceding studies. If crystallisation occurs, it serves to concentrate the volatiles in the melt, and to alter the melt composition. Care must be taken to utilise the correct *melt* composition and volatile inventory when using any solubility model. We provide an example of such a calculation in Section 5.1. The same applies to the precipitation of an immiscible sulphide phase, which must also be accounted for independently to the application of SolEx.

5. Application of SolEx

SolEx is available for Mac OS X, and Windows machines. The user specifies P, T conditions, redox condition (as ΔNNO), melt composition and total (initial) volatile contents. The melt composition can be entered as the mass proportions (wt%) of 7-components; SiO_2, Al_2O_3, CaO, K_2O, Na_2O, MgO, FeO. Note that Fe_2O_3 does not feature in the parameterisation. Alternatively, the simplified compositional parameterisation of Dixon et al. (1997) can be used, and the composition simply entered as the weight fraction of SiO_2. (Note that this one-component has only been tested for one suite of North Arch basalts, Dixon et al., 1997.) The model is applicable for basalts with <53 wt% SiO_2.

Closed-system degassing, where the vapour and melt are assumed to remain in equilibrium at all depths, and open-system behaviour, where the vapour is lost (or chemically isolated) from the melt immediately upon exsolution, can both be modelled. The output includes dissolved H_2O, CO_2, S and Cl concentrations as functions of pressure. Fig. 5 illustrates example outputs for melts of St8.1 and MAS1 compositions. Mass and molar proportions of the fluid, together with the fluid volume percentage, are also calculated. The output is in the form of a tab delimited text file, SolEx_output.txt, that is written to the directory from which SolEx was run (Windows) or to the Desktop (OS X). Upon clicking the Isobars button, H_2O–CO_2 isobars are calculated at 4, 3, 2, 1, 0.5 and 0.25 kbar for the selected melt composition, and output as SolEx_isobars.txt. These output files can be opened in any spreadsheet or text editor, and further calculations or graphical plots performed from third party programs.

5.1. An example application: Stromboli degassing

To illustrate the utility of SolEx in modelling volcanic degassing processes, we calculate S and Cl concentrations in a basalt. Métrich et al. (2010) studied a Ca-rich Stromboli basalt, and calculated a crystallisation path. We use their pumice sample ST82 as a test case; melt fractions, F, and associated melt compositions are given in Table 3. Métrich et al. (2010) used the CO_2–H_2O composition of the melt to estimate the pressure of melt inclusion entrapment. However, such an approach assumes that the included melts are saturated in volatiles, an assumption that is difficult to verify in

Table 3
Melt compositions (in wt%) for Stromboli pumice sample ST82 calculated for varying melt fractions, i.e. crystal contents up to 19%, after Métrich et al. (2010). Data taken from their Table 2. FeO_T signifies total Fe, cast as FeO.

F (%)	SiO_2	Al_2O_3	FeO_T	MgO	CaO	Na_2O	K_2O	Π	$[H_2O]_0$	$[CO_2]_0$	$[S]_0$	$[Cl]_0$
100	48.6	14.7	7.2	8.3	13.1	2.2	1.6	0.913	2.20	2900	3500	1500
96.7	48.5	14.9	7.3	8.0	12.9	2.2	1.6	0.838	2.28	2999	3619	1551
89.2	48.4	15.8	7.4	7.3	12.1	2.4	1.8	0.631	2.47	3251	3924	1682
84.9	48.3	16.4	7.4	6.8	11.6	2.5	1.9	0.478	2.59	3416	4122	1767
81.0	48.2	16.9	7.4	6.3	11.1	2.6	2.0	0.332	2.72	3580	4321	1852

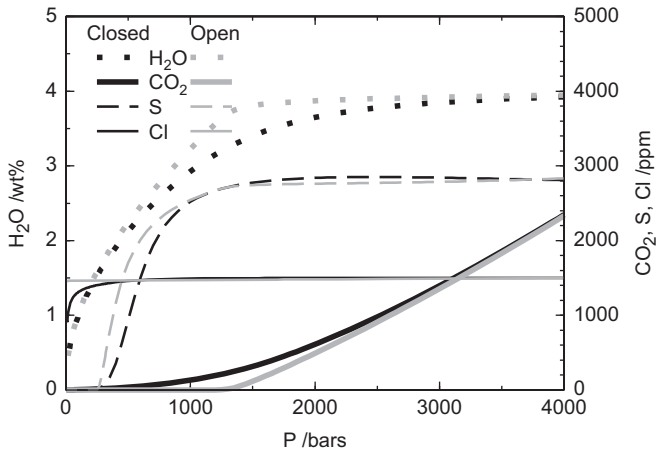

Fig. 7. Comparison of open- and closed-system calculations, performed on a basalt of OIB composition (Table 1) at $T=1150\,^{\circ}C$ with initial volatile contents $H_2O=4$ wt%, $CO_2=5000$ ppm, $S=3000$ ppm, $Cl=1500$ ppm. In open-system conditions, the CO_2-rich fluid generated at high pressures is immediately lost, meaning that less H_2O dissolves in the fluid and H_2O concentrations remain higher.

convecting systems such as Stromboli (Witham, 2011a,b). In order to avoid this assumption, we model the evolution of volatile concentrations within the melts by performing closed-system degassing profiles given the full range of crystallinities and corresponding melt compositions given in Table 3. We assume that all four volatile species behave incompatibly, such that the total mass of each volatile component in the melt plus gas is increased by a factor of $1/F$.

When crystallisation is accounted for, we can model almost all the S and Cl melt inclusion data as being due to the closed-system degassing with simultaneous crystallisation of up to 19% by assuming starting volatile content $[i]_0$ of $[H_2O]_0=2.2$ wt%, $[CO_2]_0=2900$ ppm, $[S]_0=3500$ ppm and $[Cl]_0=1500$ ppm (Fig. 8a,b). However, Fig. 8c shows that such a simple model cannot explain the H_2O contents of the melt inclusions. These trends have been previously explained to be due to buffering by a CO_2-rich fluid fluxing through the system (e.g. Rust et al., 2004; Métrich et al., 2010; Blundy et al., 2010), diffusion of H_2O through the host crystal (Gonnermann and Manga, 2005) or mixing between volatile-rich and volatile-poor magmas (Witham, 2011a,b).

Fig. 9 shows that the S/Cl ratio of the fluid phase is highly dependent on pressure. Assuming that emitted gases represent an equilibrium fluid from some depth, it is therefore possible to deduce the pressure of equilibration of a gas emitted from a volcano from the S/Cl or CO_2/S ratio, as previously noted by Burton et al. (2007). SolEx provides a simple platform on which to perform such analysis.

6. Summary

SolEx is a computer program, written to run under OS X and Windows, that predicts the behaviour of mixed COHSCl fluids in basaltic (<53 wt% SiO_2, amphibole absent) systems based on the models of Dixon (1997) for H_2O–CO_2 behaviour in basalt, the Churakov and Gottschalk (2003a,b) equation of state for non-ideal behaviours of sulphate and chloride in the fluid phase, and a parameterisation of experiments from Lesne et al. (2011a) for S and Cl partitioning between basaltic melt and a coexisting fluid phase. H_2S partitioning is not modelled due to an absence of relevant data, so SolEx is only applicable under conditions of oxygen fugacity greater than 0.5log units above the nickel–nickel oxide (NNO) buffer.

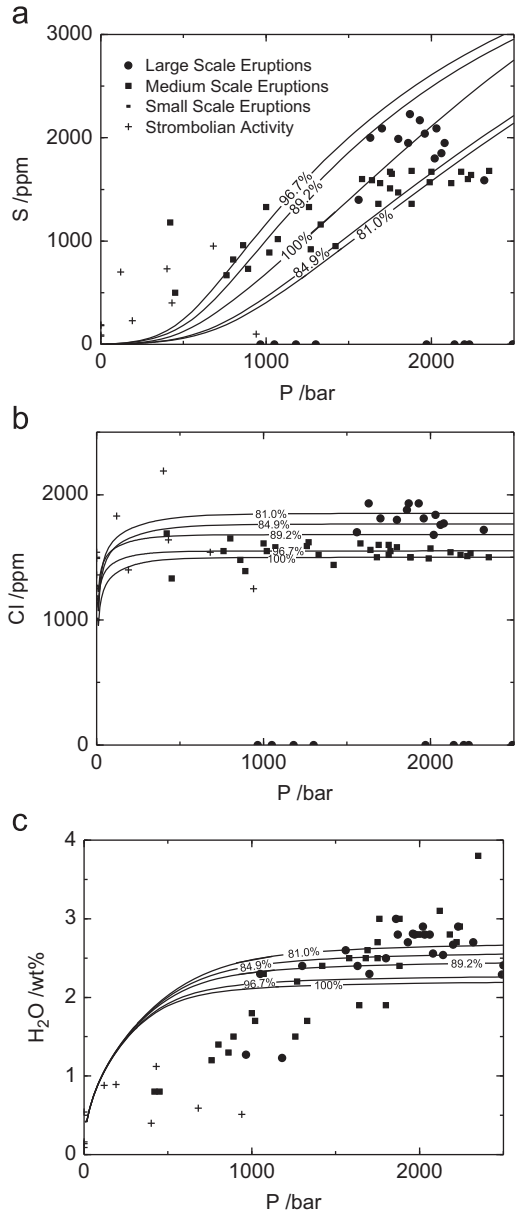

Fig. 8. A comparison of SolEx model results with data from Métrich et al. (2010), allowing for $<20\%$ crystallisation of the melt. Model compositions are those calculated from the crystallisation path by Métrich et al. (2010) and are given in Table 3. Melt inclusion data are from Métrich et al. (2010), supplementary data Table 1. Crystallisation can account for variability in S and Cl concentrations, but not trends in H_2O concentration.

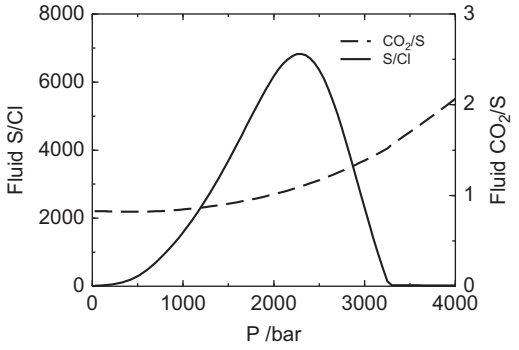

Fig. 9. S/Cl and CO_2/S ratios in the fluid phase as a function of pressure, for the bulk composition of Métrich et al. (2010) (Table 3). Fluid composition is strongly dependent on pressure.

SolEx can be used to predict degassing behaviour in both open- and closed-systems. Designed for use on basaltic systems, we find that SolEx performs well compared to other models for tholeiitic and calc-alkaline basalts, and matches relevant experimental data well. Given the relative lack of constraint on the compositional and temperature dependencies of S and Cl partitioning, we advise caution when applying SolEx to conditions far from those of its calibration. We hope to improve the range of calibration of the model in future releases.

Acknowledgements

We kindly thank R. Moretti and J. Lowenstern for insightful reviews that added to the clarity and completeness of the manuscript, and P. Papale for supplying the code for the model of Papale et al. (2006). T. Lei (http://hxxland.com) designed the SolEx logo and generously authorised its use. This research was funded by NERC grant NE/F004222/1.

Appendix A. Supplementary data

Supplementary data associated with this article can be found in the online version at doi:10.1016/j.cageo.2011.09.021.

References

Aiuppa, A., 2009. Degassing of halogens from basaltic volcanism: insights from volcanic gas observations. Chemical Geology 263, 99–109.
Aiuppa, A., Federico, C., Giudice, G., Giuffrida, G., Guida, R., Gurrieri, S., Liuzzo, M., Moretti, R., Papale, P., 2009. The 2007 eruption of Stromboli volcano: insights from real-time measurement of the volcanic gas plume CO_2/SO_2 ratio. Journal of Volcanology and Geothermal Research 182, 221–230.
Aiuppa, A., Federico, C., Giudice, G., Gurrieri, S., Paonita, A., Valenza, M., 2004. Plume chemistry provides insights into mechanisms of sulfur and halogen degassing in basaltic volcanoes. Earth and Planetary Science Letters 222, 469–483.
Aiuppa, A., Moretti, R., Federico, C., Giudice, G., Gurrieri, S., Liuzzo, M., Papale, P., Shinohara, H., Valenza, M., 2007. Forecasting Etna eruptions by real-time observation of volcanic gas composition. Geology 35, 1115–1118.
Allard, P., Carbonelle, J., Métrich, N., Loyer, H., Zettwoog, P., 1994. Sulphur output and magma degassing budget of Stromboli volcano. Nature 368, 326–330.
Alletti, M., Baker, D.R., Scaillet, B., Aiuppa, A., Moretti, R., Ottolini, L., 2009. Chlorine partitioning between a basaltic melt and H_2O–CO_2 fluids at Mount Etna. Chemical Geology 263, 37–50.
Belonoshko, A.B., Shi, P., Saxena, S.K., 1992. SUPERFLUID: a FORTRAN-77 program for calculation of Gibbs free energy and volume of C–H–O–N–S–Ar mixtures. Computers and Geosciences 18, 1267–1269.
Blundy, J.D., Cashman, K.V., Rust, A., Witham, F., 2010. A case for CO_2-rich arc magmas. Earth and Planetary Science Letters 290, 289–301.
Botcharnikov, R., Holtz, F., Behrens, H., 2007. The effect of CO_2 on the solubility of H_2O–Cl fluids in andesitic melt. European Journal of Mineralogy 19, 671–680.
Botcharnikov, R.E., Behrens, H., Holtz, F., Koepke, J., Sato, H., 2004. Sulfur and chlorine solubility in Mt. Unzen rhyodacitic melt at 850 °C and 200 mPa. Chemical Geology 213, 207–225.
Burnham, C.W., 1979. Magmas and hydrothermal fluids. In: Barnes, H.L. (Ed.), Geochemistry of Hydrothermal Ore Deposits. Wiley-Interscience, pp. 71–136.
Burton, M., Allard, P., Murè, F., La Spina, A., 2007. Magmatic gas composition reveals the source depth of slug driven Strombolian explosive activity. Science 317, 227–230.
Carroll, M.R., 2005. Chlorine solubility in evolved alkaline magmas. Annals of Geophysics 48, 619–631.
Chevychelov, V.Y., Botcharnikov, R., Holtz, F., 2008. Experimental study of chlorine and fluorine partitioning between fluid and subalkaline basaltic melt. Doklady Earth Sciences 422, 1089–1092.
Churakov, S.V., Gottschalk, M., 2003a. Perturbation theory based equation for polar molecular fluids: II. Fluid mixtures. Geochimica et Cosmochimica Acta 67, 2415–2425.
Churakov, S.V., Gottschalk, M., 2003b. Perturbation theory based equation of state for polar molecular fluids: I. Pure fluids. Geochimica et Cosmochimica Acta 67, 2397–2414.
Collins, S.J., Pyle, D.M., Maclennan, J., 2009. Melt inclusions track pre-eruption storage and dehydration of magmas at Etna. Geology 37, 571–574.
Dixon, J.E., 1997. Degassing of alkalic basalts. American Mineralogist 82, 368–378.
Dixon, J.E., Clague, D.A., Stolper, E.M., 1991. Degassing history of water, sulfur and carbon dioxide in submarine lavas from Kilauea volcano, Hawaii. Journal of Geology 99, 371–394.
Dixon, J.E., Clague, D.A., Wallace, P., Poreda, R., 1997. Volatiles in alkalic basalts from the north arch volcanic field, Hawaii: extensive degassing of deep submarine-erupted alkalic series lavas. Journal of Petrology 38, 911–939.
Dixon, J.E., Stolper, E., Holloway, J.R., 1995. An experimental study of water and carbon dioxide solubilities in mid-ocean ridge basaltic liquids. Part I: calibration and solubility models. Journal of Petrology 36, 1607–1631.
Dixon, J.E., Stolper, E.M., 1995. An experimental study of water and carbon dioxide solubilities in mid-ocean ridge basaltic liquids. Part II: applications to degassing. Journal of Petrology 36, 1633–1646.
Edmonds, M., Gerlach, T.M., 2007. Vapor segregation and loss in basaltic melts. Geology 35, 751–754.
Francis, P., Burton, M.R., Oppenheimer, C., 1998. Remote measurements of volcanic gas compositions by solar occultation spectroscopy. Nature 396, 567–570.
Gonnermann, H.M., Manga, M., 2005. Nonequilibrium magma degassing: results from modeling of the ca. 1340 A.D. eruption of Mono Craters, California. Earth and Planetary Science Letters 238, 1–16.
Hauri, E., 2002. SIMS analysis of volatiles in silicate glasses, 2: isotopes and abundances in Hawaiian melt inclusions. Chemical Geology 183, 115–141.
Holloway, J.R., 1977. Fugacity and activity of molecular species in supercritical fluids. In: Fraser, D. (Ed.), Thermodynamics in Geology. Reidel, Boston, pp. 161–181.
Holloway, J.R., Blank, J.G., 1994. Experimental results applied to C–O–H in natural melts. In: Carroll, M.R., Holloway, J.R. (Eds.), Volatiles in Magmas. Reviews in Mineralogy 30, 187–230.
Horton, K.A., Williams-Jones, G., Garbeil, H., Elias, T., Sutton, A.J., Mouginis-Mark, P.J., Porter, J.N., Clegg, S., 2006. Real-time measurement of volcanic SO_2 emissions: validation of a new UV correlation spectrometer (FLYSPEC). Bulletin of Volcanology 68, 323–327.
Jugo, P.J., Luth, W.R., Richards, J.P., 2005. An experimental study of the sulfur content in basaltic melts saturated with immiscible sulfide or sulfate liquids at 1300 °C and 1.0 GPa. Journal of Petrology 46, 783–798.
Jugo, P.J., Wilke, M., Botcharnikov, R., 2010. Sulfur K-edge XANES analysis of natural and synthetic basaltic glasses: implications for S speciation and S content as function of oxygen fugacity. Geochimica et Cosmochimica Acta 74, 5926–5938.
Keppler, H., 2010. The distribution of sulfur between haplogranitic melts and aqueous fluids. Geochimica et Cosmochimica Acta 74, 645–660.
Kilinc, A., Carmichael, I.S.E., Rivers, M.L., Sack, R.O., 1983. The ferric–ferrous ratio of natural silicate liquids equilibrated in air. Contributions to Mineralogy and Petrology 83, 136–140.
Lesne, P., Kohn, S.C., Blundy, J.D., Witham, F., Botcharnikov, R., Behrens, H., 2011a. Experimental simulation of closed-system degassing in the system basalt–H_2O–CO_2–S–Cl. Journal of Petrology 52, 1737–1762.
Lesne, P., Scaillet, B., Pichavant, M., Beny, J.-M., 2011b. The carbon dioxide solubility in alkali basalts: an experimental study. Contributions to Mineralogy and Petrology 162, 153–168. doi:10.1007/s00410-010-0585-0.
Lesne, P., Scaillet, B., Pichavant, M., Iacono-Marziano, G., Beny, J.-M., 2011c. The H_2O solubility of alkali basaltic melts: an experimental study. Contributions to Mineralogy and Petrology 162, 133–151. doi:10.1007/s00410-010-0588-x.
Liu, Y., Samaha, N.-T., Baker, D.R., 2007. Sulfur concentration at sulfide saturation (SCSS) in magmatic silicate melts. Geochimica et Cosmochimica Acta, 1783–1799.
Martin, R.S., Sawyer, G.M., Spampinato, L., Salerno, G.G., Ramirez, C., Ilyinskaya, E., Witt, M.L.I., Mather, T.A., Watson, I.M., Phillips, J.C., Oppenheimer, C., 2010. A total volatile inventory for Masaya volcano, Nicaragua. Journal of Geophysical Research 115, B09215.
Métrich, N., Bertagnini, A., DiMuro, A., 2010. Conditions of magma storage, degassing and ascent at Stromboli: new insights into the volcano plumbing system with inferences on the eruptive dynamics. Journal of Petrology 51, 603–626.
Métrich, N., Bertagnini, A., Landi, P., Rosi, M., 2001. Crystallisation driven decompression and water loss at Stromboli volcano (Aeolian Islands, Italy). Journal of Petrology 42 (8), 1471–1490.
Métrich, N., Rutherford, M.J., 1992. Experimental study of chlorine behaviour in hydrous silicic melts. Geochimica et Cosmochimica Acta 56, 607–616.
Millan, M.M., Townsend, S., Davies, J., 1969. Study of the Barringer Refractor Plate Correlation Spectrometer as a Remote Sensing Instrument. Technical Report. University of Toronto.
Moore, G., 2008. Interpreting H_2O and CO_2 contents in melt inclusions: constraints from solubility experiments and modeling. In: Putirka, K., Tepley III, F. (Eds.), Minerals, Inclusions and Volcanic Processes, Reviews in Mineralogy and Geochemistry 69, 333–361.
Moore, G., Vennemann, T., Carmichael, I.S.E., 1998. An empirical model for the solubility of H_2O in magmas to 3 kbars. American Mineralogist 83, 36–42.
Moretti, R., Baker, D.R., 2008. Modeling the interplay of fO_2 and fS_2 along the FeS-silicate melt equilibrium. Chemical Geology 256, 286–298.
Moretti, R., Ottonello, G., 2005. Solubility and speciation of sulfur in silicate melts: the conjugated Toop–Samis–Flood–Grjotheim (CTSFG) model. Geochimica et Cosmochimica Acta 69, 801–823.
Moretti, R., Papale, P., 2004. On the oxidation state and volatile behaviour on multicomponent gas–melt equilibria. Chemical Geology 213, 265–280.

Moretti, R., Papale, P., Ottonello, G., 2003. A model for the Saturation of C–O–H–S Fluids in Silicate Melts, vol. 213. Geological Society, London (Special Publications), pp. 81–101.
Moune, S., Holtz, F., Botcharnikov, R., 2009. Sulphur solubility in andesitic to basaltic melts: implications for Hekla volcano. Contributions to Mineralogy and Petrology 157, 691–707.
Newman, S., Lowenstern, J.B., 2002. VOLATILECALC: a silicate melt–H_2O–CO_2 solution model written in Visual Basic for Excel. Computers and Geosciences 28, 597–604.
Pan, V., Holloway, J.R., Hervig, R.L., 1991. The pressure and temperature dependence of carbon dioxide solubility in tholeiitic basalt melts. Geochimica et Cosmochimica Acta 55, 1587–1595.
Papale, P., 1999. Modeling of the solubility of a two-component H_2O+CO_2 fluid in silicate liquids. American Mineralogist 84, 477–492.
Papale, P., Moretti, R., Barbato, D., 2006. The compositional dependence of the saturation surface of H_2O+CO_2 fluids in silicate melts. Chemical Geology 229, 78–95.
Pichavant, M., Di Carlo, I., Le Gac, Y., Rotolo, S.G., Scaillet, B., 2009. Experimental constraints on the deep magma feeding system at Stromboli volcano, Italy. Journal of Petrology 50, 601–624.
Pino, N.A., Moretti, R., Allard, P., Boschi, E., 2011. Seismic precursors of a basaltic paroxysmal explosion track deep gas accumulation and slug upraise. Journal of Geophysical Research 116, B02312.
Platt, U., 1994. Differential optical absorption spectroscopy (doas). In: Sigrist, M.W. (Ed.), Air Monitoring by Spectroscopic Techniques. Chemical Analysis Series, vol. 127. Wiley & Sons, pp. 27–84.
Presnell, D.C., Hoover, J., 1987. High pressure phase equilibrium constraints on the origin of mid-ocean ridge basalts. In: Mysen, B.O. (Ed.), Magmatic Processes: Physiochemical Principles, vol. 1. Geochemical Society, pp. 75–89.
Rust, A.C., Cashman, K.V., Wallace, P.J., 2004. Magma degassing buffered by vapor flow through brecciated conduit margins. Geology 32, 349–352.
Sadofsky, S.J., Portnyagin, M., Hoernle, K., van den Bogaard, P., 2008. Subduction cycling of volatiles and trace elements through the Central American volcanic arc: evidence from melt inclusions. Contributions to Mineralogy and Petrology 155, 433–456.
Scaillet, B., Clemente, B., Evans, B.W., Pichavant, M., 1998. Redox control of sulfur degassing in silicic magmas. Journal of Geophysical Research 103 (B10), 23937–23949.
Scaillet, B., Pichavant, M., 2005. A model of sulphur solubility for hydrous mafic melts: application to the determination of magmatic fluid compositions of Italian volcanoes. Annals of Geophysics 48, 671–698.
Shinohara, H., 2009. A missing link between volcanic degassing and experimental studies on chloride partitioning. Chemical Geology 263, 51–59.
Shishkina, T.A., Botcharnikov, R.E., Holtz, F., Almeev, R.R., Portnyagin, M.V., 2010. Solubility of H_2O- and CO_2-bearing fluids in tholeiitic basalts at pressures ip to 500 MPa. Chemical Geology 277, 115–125.
Shmulovich, K.I., Graham, C.M., 2004. An experimental study of phase equilibria in the systems H_2O–CO_2–$CaCl_2$ and H_2O–CO_2–NaCl at high pressures and temperatures (500–800 °C, 0.5–0.9 GPa): geological and geophysical applications. Contributions to Mineralogy and Petrology 146, 450–462.
Silver, L.A., Stolper, E., 1989. H_2O in albitic glasses. Journal of Petrology 74, 55–66.
Spilliaert, N., Allard, P., Métrich, N., Sobolev, A.V., 2006a. Melt inclusion record of the conditions of ascent, degassing, and extrusion of volatile-rich alkali basalt during the powerful 2002 flank eruption of Mount Etna (Italy). Journal of Geophysical Research 111, B04203.
Spilliaert, N., Métrich, N., Allard, P., 2006b. S–Cl–F degassing pattern of water-rich alkali basalt: modelling and relationship with eruption styles on Mount Etna volcano. Earth and Planetary Science Letters 248, 772–786.
Stelling, J., Botcharnikov, R., Beerman, O., Nowak, M., 2008. Solubility of H_2O- and chlorine-bearing fluids in basaltic melt of Mount Etna at $T=1050$–1250 °C and $P=200$ MPa. Chemical Geology 256, 102–110.
Vetere, F.P., Botcharnikov, R., Holtz, F., Behrens, H., De Rosa, R., 2011. Solubility of H_2O and CO_2 in shoshonitic melts and 1250 °C and pressures from 50 to 400 MPa: Implications for Campi Flegrei magmatic systems. Journal of Volcanology and Geothermal Research 202, 251–261. doi:10.1016/j.jvolgeores.2011.03.002.
Wallace, P., Carmichael, I.S.E., 1992. Sulfur in basaltic melts. Geochimica et Cosmochimica Acta 56, 1863–1874.
Webster, J.D., 1997. Chloride solubility in felsic melts and the role of chloride in magmatic degassing. Journal of Petrology 38, 1793–1807.
Webster, J.D., 2004. The exsolution of magmatic hydrosaline chloride liquids. Chemical Geology 210, 33–48.
Webster, J.D., de Vivo, B., 2002. Experimental and modeled solubilities of chlorine in aluminosilicate melts, consequences of magma evolution, and implications for exsolution of hydrous chloride melt at Mt. Somma-Vesuvius. American Mineralogist 87, 1046–1061.
Webster, J.D., Kinzler, R.J., Mathez, E.A., 1999. Chloride and water solubility in basalt and andesite melts and implications for magmatic degassing. Geochimica et Cosmochimica Acta 63, 729–738.
Webster, J.D., Rebbert, C.R., 1998. Experimental investigation of H_2O and Cl solubilities in F-enriched silicate liquids: implications for volatile saturation of topaz rhyolite magmas. Contributions to Mineralogy and Petrology 132, 198–207.
Webster, J.D., Sintoni, M.F., de Vivo, B., 2009. The partitioning behavior of Cl, S and H_2O in aqueous vapor- $\pm$saline-liquid saturated phonolitic and trachytic melts at 200 MPa. Chemical Geology 263, 19–36.
Witham, F., 2011a. Conduit convection, magma mixing, and melt inclusion trends at persistently degassing volcanoes. Earth and Planetary Science Letters 301, 345–352.
Witham, F., 2011b. Conduit convection, magma mixing, and melt inclusion trends at persistently degassing volcanoes: reply to comment by Métrich et al. (2011). Earth and Planetary Science Letters 306, 309–311.
Workman, R.K., Hart, S.R., 2005. Major and trace element composition of the depleted MORB mantle (DMM). Earth and Planetary Science Letters 231, 53–72.
Yoder, H.S., Tilley, C.E., 1962. Origin of basalt magmas: an experimental study of natural and synthetic rock systems. Journal of Petrology 3 (3), 342–532.